Journal of Experimental Botany, Vol. 65, No. 9, pp. 2243–2256, 2014
doi:10.1093/jxb/eru089 Advance Access publication 22 March, 2014
This paper is available online free of all access charges (see http://jxb.oxfordjournals.org/open_access.html for further details)

Journal of Experimental Botany
www.jxb.oxfordjournals.org

RESEARCH PAPER

Transcriptional and hormonal regulation of petal and stamen development by *STAMENLESS*, the tomato (*Solanum lycopersicum* L.) orthologue to the B-class *APETALA3* gene

Muriel Quinet[1,*], Gwennaël Bataille[1], Petre I. Dobrev[2], Carmen Capel[3], Pedro Gómez[3,†], Juan Capel[3], Stanley Lutts[1], Václav Motyka[2], Trinidad Angosto[3] and Rafael Lozano[3]

[1] Groupe de Recherche en Physiologie végétale, Earth and Life Institute, Université catholique de Louvain, Croix du Sud 4–5 bte L7.07.13, B-1348 Louvain-la-Neuve, Belgium
[2] Institute of Experimental Botany, Academy of Sciences of the Czech Republic, Rozvojová 263, Prague 6, 16502, Czech Republic
[3] Centro de Investigación en Biotecnología Agroalimentaria (BITAL), Universidad de Almería, 04120 Almería, Spain

* To whom correspondence should be addressed. E-mail: muriel.quinet@uclouvain.be
† Present address: Instituto de Investigación y Formación Agraria y Pesquera, Autovía del Mediterráneo, 04745 La Mojonera, Almería, Spain

Received 2 January 2014; Revised 31 January 2014; Accepted 10 February 2014

Abstract

Four B-class MADS box genes specify petal and stamen organ identities in tomato. Several homeotic mutants affected in petal and stamen development were described in this model species, although the causal mutations have not been identified for most of them. In this study we characterized a strong *stamenless* mutant in the tomato Primabel cultivar (*sl-Pr*), which exhibited homeotic conversion of petals into sepals and stamens into carpels and we compared it with the *stamenless* mutant in the LA0269 accession (*sl-LA0269*). Genetic complementation analysis proved that both *sl* mutants were allelic. Sequencing revealed point mutations in the coding sequence of the *Tomato APETALA3* (*TAP3*) gene of the *sl-Pr* genome, which lead to a truncated protein, whereas a chromosomal rearrangement in the *TAP3* promoter was detected in the *sl-LA0269* allele. Moreover, the floral phenotype of *TAP3* antisense plants exhibited identical homeotic changes to *sl* mutants. These results demonstrate that *SL* is the tomato *AP3* orthologue and that the mutant phenotype correlated to the *SL* silencing level. Expression analyses showed that the *sl-Pr* mutation does not affect the expression of other tomato B-class genes, although *SL* may repress the A-class gene *MACROCALYX*. A partial reversion of the *sl* phenotype by gibberellins, gene expression analysis, and hormone quantification in *sl* flowers revealed a role of phytohormones in flower development downstream of the *SL* gene. Together, our results indicated that petal and stamen identity in tomato depends on gene–hormone interactions, as mediated by the *SL* gene.

Key words: *APETALA3*, B-class gene, flower morphogenesis, hormone regulation, *Solanum lycopersicum*, *STAMENLESS*, tomato.

Introduction

Extensive genetic and molecular studies in several model plant species have led to a broadly accepted model of flower development based on the combined activity of three functions that determine floral organ identity in the so-called ABC model (Coen and Meyerowitz, 1991). The expression of class A genes in the first floral whorl specifies sepal identity, class A and B genes combined in the second whorl specify petal identity, class B and C genes in the third whorl determine stamen identity, and C-class genes in the fourth whorl specify carpel identity. Additional regulatory functions have been added, such as class D genes that are essential for ovule identity (Colombo *et al.*, 1995) and class E genes that

Abbreviations: ABA, abscisic acid; ACC, 1-aminocyclopropane-1-carboxylic acid; Brs, brassinosteroids; BzA, benzoic acid; CK, cytokinin; GA_3, gibberellic acid 3; GAs, gibberellins; IAA, indole-3-acetic acid; JA, jasmonic acid; PA, polyamine; Pr, Primabel tomato cultivar; SA, salicylic acid; WT, wild type.

are necessary for proper floral organ identity in the different whorls (Pelaz *et al.*, 2001). In *Arabidopsis*, there are two A-class genes, known as *APETALA1* (*AP1*) and *APETALA2* (*AP2*), two B-class genes known as *APETALA3* (*AP3*) and *PISTILLATA* (*PI*), and one C-class gene named *AGAMOUS* (*AG*). The E-function genes are *SEPALLATA1* (*SEP1*), *2*, *3*, and *4* (Pelaz *et al.*, 2001). All of these genes, with the exception of *AP2* (and its homologues), are MADS box genes (Theissen *et al.*, 2000), which comprise a broad family of eukaryotic genes that encode transcription factors containing a highly conserved DNA-binding domain (MADS domain). Functional roles of many MADS box genes seem to be conserved among flowering plants, although some homologous genes in different plant species have recruited novel functions through evolutionary mechanisms currently under study (see review of Smaczniak *et al.*, 2012).

Several homologues of *Arabidopsis* homeotic genes are known in tomato (*Solanum lycopersicum* L.). *MACROCALYX* (*MC*) represents the A class and is involved in the development of sepals in the first whorl and in inflorescence determinacy (Vrebalov *et al.*, 2002). Class B MADS box genes are represented by four genes. In tomato, as in other species belonging to the 'core eudicots' clade, a gene-duplication event in the *AP3* gene subfamily led to two paralogous members (Hernandez-Hernandez *et al.*, 2007), namely, the *Tomato MADS box gene 6* (*TM6*) (syn. *TDR6*; Busi *et al.*, 2003; Pnueli *et al.*, 1991) and the *Tomato APETALA3* (*TAP3*) gene (syn. *SlDEF*, *LeAP3*; Kramer *et al.*, 1998; de Martino *et al.*, 2006). A mutation in *TAP3* and the silencing of *TM6* both resulted in the conversion of stamens into carpels and a more or less severe conversion of petals into sepals (de Martino *et al.*, 2006). Two *PI* homologues were also identified, namely *Tomato PISTILLATA* (*TPI*; de Martino *et al.*, 2006) (syn. *SlGLO2*; Mazzucato *et al.*, 2008) and *Solanum lycopersicum GLOBOSA* (*SlGLO*; Mazzucato *et al.*, 2008) (syn. *SlGLO1*, *LePI*, *TPIB*; Leseberg *et al.*, 2008; Geuten and Irish, 2010). Both *TPI*- and *TPIB*-silenced plants showed aberrant carpelloid stamens while petals appeared as wild type (Geuten and Irish, 2010). Tomato C-class gene *TOMATO AGAMOUS 1* (*TAG1*) has been identified for its role in the specification of stamen and carpel identities (Pnueli *et al.*, 1994a). In tomato, the two *SEP*-like genes (E-class) *Tomato MADS box gene 5* (*TM5*) (Pnueli *et al.*, 1994b) and *Tomato AGAMOUS-LIKE gene 2* (*TAGL2*) (syn. *TM29*; Ampomah-Dwamena *et al.*, 2002; Busi *et al.*, 2003) have been described on the basis of their expression patterns and down-regulated phenotypes. Other MADS box genes expressed during tomato reproductive development have been isolated (Busi *et al.*, 2003). *Tomato MADS box gene 4* (*TM4*) (syn. *TDR4*; Pnueli *et al.*, 1991; Busi *et al.*, 2003) is homologous to *FRUITFULL* (*FUL*) (Lozano *et al.*, 2009). The nucleotide sequences of *TAGL1* (syn. *ARLEQUIN* (*ALQ*)) and *TAGL11* genes show a high similarity to the *Arabidopsis* D-class genes *SHATTERPROOF1* (*SHP1*, *AGL1*) and *SEEDSTICK* (*STK*, *AGL11*), respectively (Busi *et al.*, 2003; Vrebalov *et al.*, 2009; Giménez *et al.*, 2010), and *TAGL2* and *TAGL12* share sequence homologies with Arabidopsis *AGL2* and *AGL12*, respectively (Busi *et al.*, 2003).

Several mutants exhibiting partial or complete homeotic transformations in the second and third floral organ whorls have been described in tomato, but the underlying genes have not been identified so far. Hafen and Stevenson (1958) described five *stamenless* (*sl*) mutants with more or less severe phenotypes and proposed that they are members of an allelic series. However, two allelic series were represented among *sl* mutants as analysed by Nash *et al.* (1985). The most investigated mutants for which petal and stamen identity were affected were *sl-2* (Sawhney and Greyson, 1973a, 1973b; Sawhney, 1983), *sl* (Gómez *et al.*, 1999), and *green pistillate* (*gpi*) (syn. *pi-2*, *pistillate 2*) (Rasmussen and Green, 1993). The petals are nearly normal in the *sl-2* mutant, whereas the stamens are twisted and distorted, bearing naked ovules (Sawhney and Greyson, 1973a). The *sl* mutant shows sepaloid petals and stamens being replaced by carpels in the third whorl (Bishop, 1954; Gómez *et al.*, 1999). The *gpi* mutant shows a strong and consistent homeotic transformation of petals into sepals and of stamens into carpels (Rasmussen and Green, 1993). Temperature conditions and plant growth regulators affect the development of *sl-2* and *sl* mutants (Sawhney, 1983; Rastogi and Sawhney, 1990; Singh *et al.*, 1992; Gómez *et al.*, 1999). Low temperatures, as well as gibberellic acid 3 (GA_3), result in a reversion of the mutant phenotype in both genotypes. In contrast, *sl-2* plants grown at high temperatures or treated with indole-3-acetic acid (IAA) possess carpel-like organs in place of twisted stamens (Sawhney and Greyson, 1973b; Sawhney, 1983). Moreover, the *sl-2* flower phenotype was associated with changes in endogenous hormonal contents (Sawhney, 1974; Rastogi and Sawhney, 1990; Singh *et al.*, 1992; Singh and Sawhney, 1998). Despite the physiological characterization of a number of these *stamenless* mutants, detailed information regarding the cloning and molecular nature of mutations responsible for *sl* mutants has not been published.

The link between floral homeotic genes and phytohormone pathways was recently addressed (reviewed Chandler, 2011). Genomic studies in *Arabidopsis* demonstrated that homeotic proteins bind thousands of target sites in the genome and regulate, among other things, the expression of various proteins involved in hormone biosynthesis and signalling (Kaufmann *et al.*, 2009; Ito, 2011). The ways in which hormones contribute to the development of each organ is partly known in *Arabidopsis*; stamen development is reliant on almost all hormones, petal development is affected by gibberellins (GAs), auxins, and jasmonic acid (JA), and gynoecium development is predominantly regulated by auxins (Chandler, 2011). Hormones control development by complex interconnected webs of cross-regulation, although examples of hormone crosstalk in floral organ development are currently not extensive (Chandler, 2011).

Our aim in this paper is to increase the otherwise fragmentary knowledge of flower morphogenesis control in tomato by identifying the mutations responsible for the *sl* phenotypes and investigating how *STAMENLESS* (*SL*) interacts with floral meristem identity genes and hormones to specify petal and stamen in tomato. We characterized for the first time the *sl* mutant identified in the Primabel cultivar (*sl-Pr*) (Philouze,

1991) showing a strong phenotype and compared it to the previously described *sl* mutant in the LA0269 accession (*sl-LA0269*) (Gómez *et al.*, 1999). Recently, the *SL* locus has been suggested to be the tomato orthologue of the B-function *DEFICIENS* (*DEF*) gene of *Antirrhinum majus* (Gómez *et al.*, 1999; Mazzucato *et al.*, 2008), although definitive evidence had not been provided to date. We confirm this orthologue's role by showing that the *sl* mutations described in Primabel and LA0269 backgrounds correspond to different alleles of the *SL* locus, which was previously named *TAP3* by de Martino *et al.* (2006). To understand the genetic and hormonal regulation of *SL* further, we investigated the expression of flower morphogenesis genes and the impact of gibberellins and auxin applications on inflorescence development in *sl-Pr*. Moreover, we quantified phytohormones in the *sl-Pr* mutant during flower development to highlight their role in flowers and, particularly, in petal and stamen development.

Materials and methods

Plant material and growth conditions

Seeds from tomato (*S. lycopersicum* Mill.) cv. Primabel (Pr) and its isogenic *stamenless* mutant (*sl-Pr*; Philouze, 1991) were obtained from the French National Institute for Agricultural Research (INRA; Montfavet, France). The seeds of the *stamenless* (*sl-LA0269*, LA0269) mutant were kindly provided by the Tomato Genetics Resource Center (University of California, Davis, CA, USA).

In Louvain-la-Neuve (Belgium; 50°39′95″ N, 04°34′03″ E), seeds were germinated at 25 °C in peat compost and seedlings were transplanted to 15 cm pots filled with the same compost, grown in a heated glasshouse with an average temperature of 20 ± 8 °C, and subjected to extra lighting provided by Philips HPLR 400 W bulbs to make a 16 h-long day at a minimum of 150 $\mu mol \cdot m^{-2} \cdot s^{-1}$ irradiance over a range of 400–700 nm. In AlmerÍa (Spain; 36°50′17″ N, 2°27′35″ W), seeds were germinated in peat compost and seedlings were directly transplanted to 30 m-long coconut fibre containers and grown under natural plastic greenhouse conditions (average temperature 20 ± 10 °C under approximately 14 h natural light). Plants were periodically fertilized with an NPK nutrient solution for which the composition depended on the fertilization requirements for each growing condition.

The *sl-Pr* and *sl-LA0269* mutants were compared in both conditions under different seasons. Histological sections, hormonal treatments, hormonal quantifications, and gene expression analysis were realized on Pr and *sl-Pr* plants grown in Louvain-la-Neuve under spring conditions while plants used for *TAP3* expression analysis (*sl-Pr*, *sl-LA0269*, and *TAP3*-silencing lines) and *in situ* hybridization (*sl-LA0269*) were grown in AlmerÍa under autumn conditions.

Histological studies

Flower buds of Pr and *sl-Pr* at different stages of development (from stage 2 to 9; Brukhin *et al.*, 2003) were fixed in 70% ethanol/acetic acid/formaldehyde (18:1:1, by volume; FAA), dehydrated in a graded ethanol series, embedded in paraffin, and sectioned at 5 µm. Serial longitudinal and transversal sections were stained with haematoxylin-fast green and observed with a light microscope.

Pollen viability was estimated according to Alexander (1969). Ten flowers and at least 200 pollen grains per stamen were analysed per treatment.

Hormonal treatments

The apical meristems of 20-day-old Pr and *sl-Pr* plants (before morphogenesis of the first inflorescence) were treated with 1 mM IAA or 0.5 or 1 mM of GA_3 with 0.02% Tween 20. Control plants were either not treated or treated with water and 0.02% Tween 20. A piece of cotton wool was placed on the shoot apex and saturated with 250 µl of solution twice a week for 3 weeks (during morphogenesis of the first inflorescences).

Hormonal quantification

Concentrations of the endogenous polyamines (PAs) and phytohormones including cytokinins (CKs), auxins (IAA), GAs, salicylic acid (SA), JA, brassinosteroids (Brs), abscisic acid (ABA), ethylene precursor 1-aminocyclopropane-1-carboxylic acid (ACC), benzoic acid (BzA), and their metabolites were determined in the inflorescences of Pr and *sl-Pr* plants at three developmental stages: flower buds <5 mm (stages 4–9; Brukhin *et al.*, 2003), green flowers before anthesis ≈5–8 mm length (stages 10–13), and flowers at anthesis (stage 20). Phytohormones were extracted with methanol/formic acid/water (15:1:4, by volume) from liquid nitrogen-frozen and homogenized tissues and were subsequently purified by using the dual-mode solid-phase method according to Dobrev and Kamínek (2002). Two phytohormone fractions were obtained; fraction A contained the acidic and neutral hormones (auxins, GAs, SA, JA, Brs, ABA, BzA) and fraction B contained the basic hormones (CKs, ACC). The hormonal analysis and quantification were performed by HPLC (Ultimate 3000, Dionex, Sunnyvale, CA, USA) coupled to a hybrid triple quadrupole/linear ion trap mass spectrometer (3200 Q TRAP; Applied Biosystems, Foster City, CA, USA) using a multilevel calibration graph with ^2H-labelled internal standards (as described in detail by Dobrev and Vankova, 2012; Djilianov *et al.*, 2013).

Free PAs were extracted twice with 4% $HClO_4$ (v/v) at 4 °C and derivatized by dansylation as described by Lefèvre *et al.* (2001). Samples were re-suspended in methanol, filtered (Chromafil PES-45/15, 0.45 µm; Macherey-Nagel, Düren, Germany) and injected onto a Nucleodur C_{18} Pyramid column (125 × 4.6 mm internal diameter, 5 µm particle size; Macherey-Nagel) maintained at 40 °C. Analyses were performed by a Shimadzu HPLC system coupled to a RF-20A fluorescence detector (Shimadzu, 's-Hertogenbosch, The Netherlands) with an excitation wavelength of 340 nm and an emission wavelength of 510 nm. The mobile phase consisted of a water/acetonitrile gradient from 40 to 100% acetonitrile and the flow was 1.0 $ml \cdot min^{-1}$.

Molecular identification of sl *mutations*

For the mutation identification, three independent PCR fragments—corresponding to the complete coding sequence—of *TAP3*, *TM6*, *TPI*, and *TPIB* amplified from Pr and *sl-Pr* cDNA were obtained by using the primers listed in Table 1 and then cloned into pCRII-TOPO (TOPO TA Cloning Kit; Invitrogen, Carlsbad, CA, USA) and sequenced. The *sl-Pr* mutation in the *TAP3* coding sequence resulted in the generation of a *Rse*I restriction site and a cleaved amplified polymorphic sequence (CAPS) marker was designed using the PCR conditions and primers SlmutF and R as described in Table 1 [722 bp fragment in wild type (WT), 522 + 200 bp fragments in *sl-Pr*] to identify heterozygous plants for *sl-Pr*.

The promoter sequences flanking the *TAP3* transcribed sequences in the *sl-LA0269* mutant allele were isolated by anchor-PCR as described by Schupp *et al.* (1999) with minor modifications. Cloning experiments were repeated twice with different sets of gene-specific primers and restriction enzymes to corroborate the specificity of the cloned sequences. Additionally, PCR experiments were performed with specific primers for the *sl-LA0269* promoter sequence in combination with primers for the *TAP3* coding sequence to confirm the results obtained by anchor-PCR. Heterozygote plants were identified by PCR using Sl-MutF and Sl-both primers (1019 bp fragment corresponding to the *sl-LA0269* allele) and the Sl-WTF and Sl-both primers (1185 bp fragment corresponding to the WT allele), respectively (Table 1).

Table 1. *List of primers and amplification conditions used for semi-quantitative RT-PCR expression analysis, coding sequence sequencing and cleaved amplified polymorphic sequence (CAPS) marker development*

Gene name	GenBank accession no.	Primer sequences	T_m	No. of cycles
ACTIN	U60480	actF (ATTCCCTGACTGTTTGCTAGT)	55 °C	28
		actR (TCCAACACAATACCGGTGGT)		
TAP3	DQ674532	TAP3F (ATGGCTCGTGGTAAGATCCAG)	55 °C	28
		TAP3R (TCAACCTAGAGCAAAAGTAG)		
TM6	AY098734	TM6F (GGAAAAATTGAGATCAAGAAG)	55 °C	28
		TM6R (TCAGGAGAGACGTAGATCAC)		
TPI	DQ674531	TPIF (TGGGGAGAGGTAAAATAGAG)	50 °C	28
		TPIR (GTAGATTTGGCTGCATTGGC)		
TPIB	XM004245154	TPIBF (GAATTCTCGTCTACTTCTTTGG)	55 °C	30
		TPIBR (TGCTTGCTATCTCTAGTTGTC)		
TAG1	AY098733	TAG1F (ACGCTGAAGTTGCTTTGGTT)	55 °C	28
		TAG1R (ATGAACTCCCTGGCATCAAG)		
MC	AF448521	MCF (CAGGAAAACTGGAGCTTGGA)	60 °C	28
		MCR (TCCTCCTTGCTTCTGCTACTTC)		
TM4	AY098732	TM4F (CTCGAAACGTCGATCTGGTT)	60 °C	29
		TM4R (CCTTCTTCGAAAGCTGGTTG)		
TM5	X60758	TM5F (ACAGGCAAGTGACCTTTGCT)	60 °C	28
		TM5R (TCTGTTGGCTTCGTTCAATG)		
TAGL2	AY098738	TAGL2F (GCACGAGCAATATGCTCAAA)	55 °C	28
		TAGL2R (ATCGTACCCAATTTGCAAGG)		
TAP3 (CAPS marker)	DQ674532	SlmutF (GATCGATCCCCATGTTTTGA)	60 °C	
		SlmutR (CGAGGGTCAATTGAAGGAAA)		
TAP3 (*sl-LA0269*)		Sl_MutF (CGATGAAGAGCAATGGGTTT)	60 °C	
		Sl_bothR (GGACAGATCGATGTGGGACT)		
		Sl_WtF (GCCGTGCAAGTAATCACAAA)		

Agrobacterium-*mediated transformation of tomato plants*

Silencing lines were generated by expressing an antisense *TAP3* gene construct in tomato cv. Moneymaker plants. For this purpose, a 412 bp cDNA fragment was amplified from the pPG06 plasmid with primers sl5′B forward (AAACCAAACAAATAGGCAAGTGACT) and sl3′B reverse (AGTTTCAATCTGATTGCCAATCACC). This fragment was cloned in an antisense orientation between the *Bam*HI and *Kpn*I restriction sites of a pROK II binary vector (Baulcombe *et al.*, 1986) under the control of a cauliflower mosaic virus 35S promoter (CaMV 35S). The plasmid was subsequently electroporated into *Agrobacterium tumefaciens* LBA 4404 strain for further use in genetic transformation experiments as described by Ellul *et al.* (2004). As a consequence, 23 kanamycin-resistant lines were generated from tissue culture. These lines were checked to determine their ploidy levels by flow cytometry (Ellul *et al.* 2004) and to confirm the presence of the transgene by standard PCR assays. In addition, the *TAP3* expression levels in antisense lines were analysed by reverse transcription PCR as described in the next paragraph. As a result, 14 primary diploid transgenic lines were selected and six to eight clonal replicates per line were propagated for further phenotypic analyses. Plants were acclimated in 1 l pots over 2–3 months and then transplanted to 35 l pots containing a sphagnum peat/vermiculite substrate mixture (3:1, w/w). The plants were evaluated over three consecutive years for morphological changes relating to flower development.

Gene expression analyses

Flowers of Pr and *sl-Pr* plants were sampled at two developmental stages: green flower buds of ≈5 mm length (stages 9–11; Brukhin *et al.*, 2003) and flowers at anthesis (stage 20). Inflorescences with one or two flowers at anthesis of Pr and *sl-Pr* were also collected after the different hormonal treatments (IAA 1 mM, GA_3 1 mM, water). Samples of different plants at same stage were pooled. Total RNA was prepared from 150 mg of material using the TRI Reagent Solution (Ambion, Austin, TX, USA) and DNase treatments were realized using RQ1 RNAse-free DNase (Promega, Leiden, The Netherlands) according to the manufacturer's instructions. Reverse transcription was performed with 1 µg of total RNA using the RevertAid H Minus First Strand cDNA Synthesis Kit (Fermentas, St. Leon-Rot, Germany) by following the manufacturer's instructions. At least three independent PCR amplifications were conducted for each gene using the primer pairs, annealing temperatures, and number of cycles presented in Table 1. Expression differences were analysed by gel densitometry using ImageJ software and expressed as relative values compared to actin expression (peak size of target gene/peak size of actin). Gene expression analyses were repeated twice on two independent cultures and gave similar results.

For *in situ* hybridization experiments, inflorescences and flower buds of WT and *sl-LA0269* at different stages of development (up to stage 8; Brukhin *et al.*, 2003) were sampled. Tissue preparation of *sl-LA0269* mutant, sectioning, and transcript detection were performed as described by Lozano *et al.* (1998). The *TAP3* cDNA in the pGEM-T vector was used as a template to synthesize digoxigenin-labelled sense and antisense RNA probes with T7 and SP6 RNA polymerases, respectively, according to the DIG RNA Labelling Kit (Roche Applied Science) instructions. To produce a negative control, sense RNA probes were hybridized with the same sections and no signals were observed under the given hybridization and detection conditions.

Statistical analysis

Normality tests were performed and no further transformation of the raw data was required. An ANOVA II (SAS 9.2) was performed to evaluate the genotype and floral stage effects on hormonal concentrations and on gene expression. Differences between means were scored for significance according to Tukey's test. Allelism cross segregations were verified by χ^2 test.

Results

stamenless *mutants exhibit homeotic conversions that affect petals and stamens*

At anthesis, WT tomato flowers usually consisted of six green sepals, six yellow petals, and a staminal cone made of six fused yellow stamens surrounding a gynoecium made of six fused green carpels (Fig. 1A, E). The *sl-Pr* mutant developed flowers with a first whorl having (usually) six green sepals, a second whorl composed of approximately six shorter sepals arising from the homeotic conversion of petals and, because of the homeotic conversion of the third whorl stamens into carpels, a gynoecium (which included the combination of whorls 3 and 4) made from the fusion of 10–12 green carpels (Fig. 1B). Small non-fused carpels and visible ovules were observed in the third whorl of approximately 10% of the *sl-Pr* mutant flowers (Fig. 1C). The floral phenotype of the *sl-LA0269* mutant was weaker than that of *sl-Pr* as petals showed a normal-like yellow colour and the conversion of stamens into carpels was not always complete, leading to the development of non-fused transformed carpels in the third whorl (Fig. 1E). Depending on the growing conditions, heterozygous plants for *sl-Pr* and *sl-LA0269* were either not distinguishable from the WT or displayed some stamen defects. In the Belgian conditions, most of the heterozygous plants resembled the WT and some plants displaying a fusion of some stamens with the style were observed (Fig. 1D). Under Spanish growing conditions, heterozygous plants showed more stamen defects, mainly for *sl-LA0269*. Indeed, heterozygous *sl-LA0269* plants exhibited a phenotype that was intermediate between the mutant and WT plants and characterized by distorted and short carpelloid stamens (Fig. 1E), which concurred with the description by Gómez *et al.* (1999). In addition, both mutants developed a variable percentage of parthenocarpic fruits made up of the carpels of whorls 3 and 4, depending on the growing conditions. The transformed organs from whorls 2 and 3 remained attached to the fruits in both mutants (Fig. 1G, H compared to Fig. 1F). Histological sections performed during flower morphogenesis demonstrated that the initiation of the floral organ primordia occurred in a similar fashion to the *sl-Pr* mutant than in the WT background (Fig. 2A–D) and differences were only visible later during floral organ differentiation and development (Fig. 2E–H), as was described by Gómez *et al.* (1999) for *sl-LA0269*. The *sl-Pr* and *sl-LA0269* mutations did not affect vegetative development, flowering time, or inflorescence architecture.

Given the phenotypic similarities between the *sl-Pr* and *sl-LA0269* mutants, allelism tests were performed by crossing heterozygote *sl-LA0269* or *sl-Pr* male parents with *sl-Pr* or

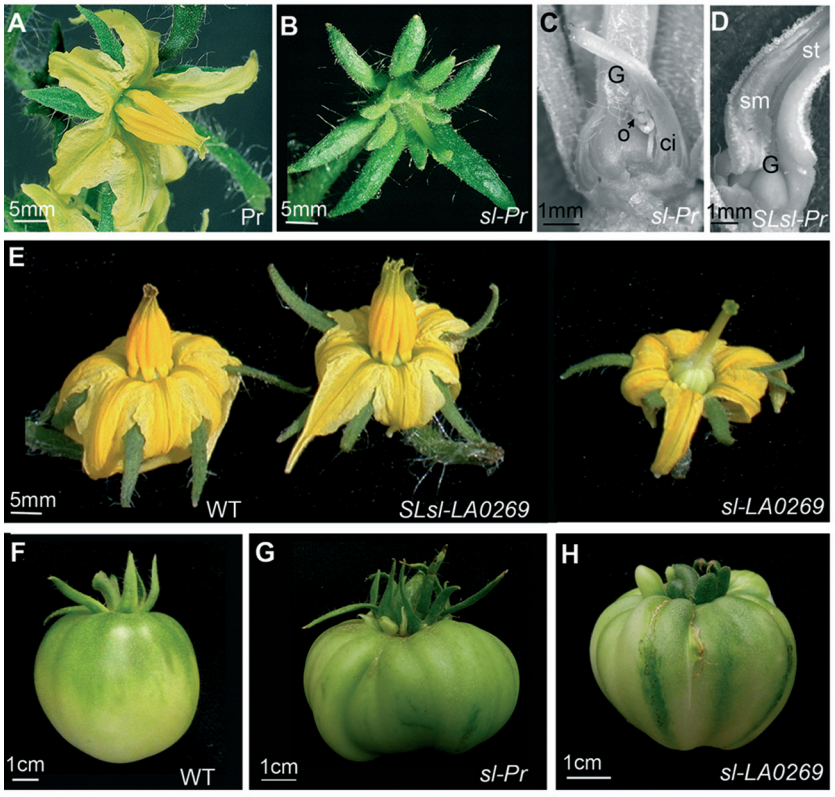

Fig. 1. Floral and fruit phenotypes of the WT tomato and *stamenless* mutants. (A–E) Flower of the (A) Pr cultivar, (B, C) *sl-Pr* mutant, (D) *SL/sl-Pr* heterozygote, (E) WT (left), heterozygote (middle), and *sl-LA0269* mutant (right). WT flowers showed five or six sepals, petals, stamens, and carpels and the *stamenless* mutant flowers showed different degrees of reversion for petals in sepals and stamens in carpels. (C, D) The inner floral whorls of a (C) *sl-Pr* flower showing non-fused carpels and visible ovules in the third whorl and (D) heterozygote flower in Pr with a stamen fused to the gynoecium. (F–H) Unripe fruits of (F) WT with the sepals of whorl 1 remaining attached to the fruit, (G) *sl-Pr* mutant with sepals of whorls 1 and 2 and non-fused carpels of whorl 3 remaining attached to the parthenocarpic fruit, and (H) *sl-LA0269* with sepals of whorl 1 and pseudo-stamens and non-fused carpels of whorl 3 remaining attached to the parthenocarpic fruit. ci, non-fused carpel; G, gynoecium; o, ovule; sm, stamen; st, style.

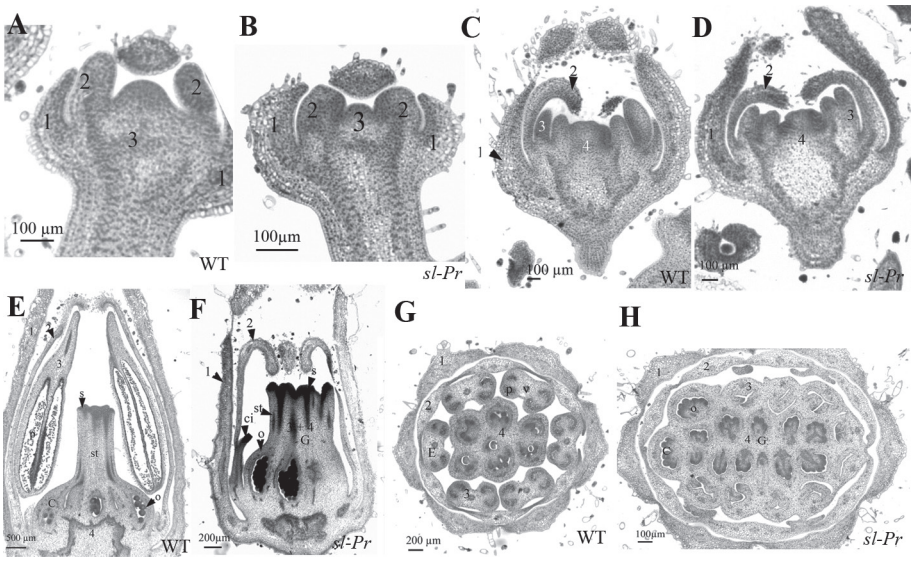

Fig. 2. Flower development of WT tomato and *stamenless* (*sl-Pr*) mutant flowers. Longitudinal (A–F) and transversal (G, H) histological sections of (A, C, E, G) WT and (B, D, F, H) *sl-Pr* mutant flower buds (A–D) initiating floral organ primordia or (E–H) having differentiated floral organs. 1–4, floral primordia or organs of first, second, third, or fourth floral whorls, respectively; C, carpel; ci, non-fused carpel; E, stamen; G, gynoecium; o, ovule; p, pollen grains; s, stigma; st, style.

sl-LA0269 mutant female parents, respectively. As a result, about half of the F_1 plants, those carrying the *sl-LA0269* and *sl-Pr* alleles simultaneously, showed a mutant phenotype, which confirmed that both mutations corresponded to *SL* locus alleles ($\chi^2 = 0.039$, $P = 0.843$).

stamenless *mutants were affected in the* TAP3 *gene*

To identify the gene affected by the *sl* mutation, the coding sequences of known tomato class B genes (*TM6*, *TAP3*, *TPI*, *TPIB*) were sequenced in Pr and *sl-Pr*. In comparison to the Pr control background, the *TM6*, *TPI*, and *TPIB* coding sequences of *sl-Pr* mutant plants were not different (data not shown), and the *TAP3* cDNA had two point mutations (Fig. 3A). The first was an A-to-T substitution in position 378 resulting in an aspartic acid instead of a glutamic acid (Fig. 3). The second change, and surely the most important one, was a nucleotide deletion in position 380 of the *TAP3* coding sequence of *sl-Pr* resulting in a frameshift mutation (Fig. 3A). The mutated allele is expected to encode a truncated protein of 161 amino acids because a stop codon in the new reading frame located 36 codons downstream from the deletion is generated by this deletion (Fig. 3B). The mutations did not affect the MADS box domain but did affect the K box and the C-terminal domains.

With regards to the *sl-LA0269* mutant, a sequence analysis of the *TAP3* full-length cDNA revealed the absence of mutations in the transcribed region, which was in agreement with previous results reported by Gómez *et al.* (1999). Therefore, we tried to clone the promoter region with PCR experiments without success. By using an anchor-PCR approach, a 2.3 kb genomic fragment located upstream of the start codon was cloned and sequenced. Molecular analysis of this fragment indicated that the promoter region of the *sl-LA0269* allele contained a proximal 1.1 kb fragment identical to that found in the WT promoter and three different small sequences of 315, 518, and 270 bp, which were not detected in the WT fragment (Fig. 3A). In the 518 bp sequence we found an *Eco*RI restriction site that generates the restriction fragment length polymorphism (RFLP) described as being tightly linked to the *SL* locus (Gómez *et al.*, 1999). Interestingly, these three sequences were homologous to others repeated in different locations of chromosome 3. Given that *TAP3* maps within chromosome 4, it is likely that a genomic rearrangement affecting the promoter region of this gene may be responsible for the mutant phenotype observed in the *sl-LA0269* mutant.

TAP3 expression was then compared in mutants, heterozygotes, and WT flowers during their development to see if the observed phenotypes were related to a decrease or absence of *TAP3* transcript abundance. Whatever the genotype, *TAP3* expression was detected in 0.5 mm-long flower buds and in flowers at anthesis (Fig. 4A). Both *sl* mutations reduced *TAP3* expression level compared to WT (Fig. 4A). In *sl-Pr*, *TAP3* transcript level was significantly reduced in both flower buds and flowers at anthesis while the expression decrease was only significant in flower buds in the *sl-LA0269* mutant. The heterozygote plants showed an intermediate *TAP3* expression level between mutant and WT plants although the difference was not significant. Given that the chromosome rearrangement found in the *TAP3* promoter region of *sl-LA0269* mutant allele likely encodes a functional SL protein, a feature which was not expected for the truncated protein detected in the *sl-Pr* allele, we analysed in depth the *TAP3* expression profile in the *sl-LA0269* mutant by *in situ* hybridization. The *TAP3* gene was expressed in the sympodial and floral meristems, as well as in young flower buds of WT inflorescences (Fig. 4B). During flower morphogenesis, *TAP3* transcripts were detected in the centre of the flower bud where the three inner floral organ whorl primordia would be subsequently initiated (Fig. 4C) and then in the organ primordia of the second and

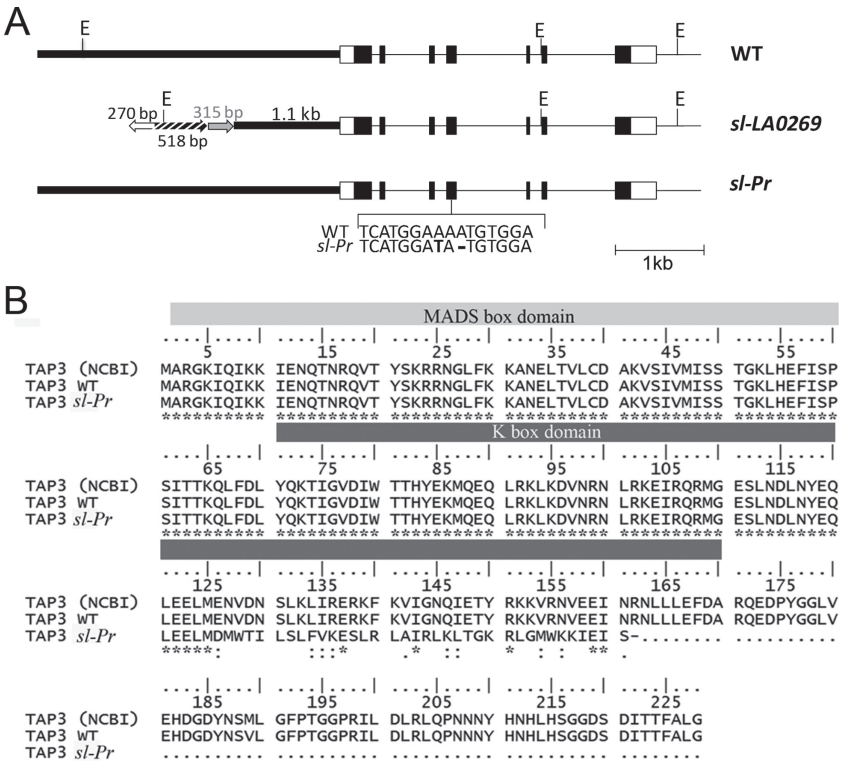

Fig. 3. Mutations in the *TAP3* sequence of the *sl-LA0269* and *sl-Pr* tomato mutants. (A) Genomic organization of the WT, *sl-LA0269*, and *sl-Pr* alleles of the *TAP3* gene. Rectangles represent exons (black sections are translated sequences whereas white ones are untranslated) and the thin line represents introns. The WT allele promoter is located in chromosome 4 and is represented by a thick black line. In the promoter of the *sl-LA0269* allele, three repeated sequences (white, grey, and striped arrows) homologous to sequences located in chromosome 3 were found 1.1 kb upstream of the transcription start site. The sequence of this 1.1 kb fragment is the same as the sequence of the WT allele promoter. The sizes of the chromosome 3 repeated sequences are indicated near the corresponding arrows and the direction of the arrow shows the corresponding sequence orientations. *Eco*RI restriction sites were used to clone both alleles, and they are also represented (E). In the *sl-Pr* allele, an A-to-T substitution and a deletion were observed in the coding sequence (fourth exon). The WT and *sl-Pr* sequences around the mutations are shown. Differences in the *sl-Pr* allele are indicated by bold characters. (B) Alignment of the amino acid sequences showing the D-to-E substitution (position 126) and the stop codon (position 162) in the *sl-Pr* mutant sequence. The MADS box and K box domains were identified by an NCBI conserved domain search (http://www.ncbi.nlm.nih.gov/Structure/cdd/wrpsb.cgi?). *TAP3* GenBank accession DQ674532.

third floral whorls (Fig. 4D). Later, during floral organ differentiation, *TAP3* was strongly expressed in the stamens and some expression was observed in the ovule primordia, when the carpels just fused (Fig. 4F). This pattern of *TAP3* expression in WT flowers is similar to what has been previously reported (de Martino *et al.*, 2006; Mazzucato *et al.*, 2008). In *sl-LA0269* inflorescences, *TAP3* was weakly expressed in the sympodial and floral meristems, whereas in the young flower buds its transcripts were detected in the meristem domains giving rise to second- and third-whorl primordia (Fig. 4E). In young flowers, *TAP3* transcripts were detected at slight levels in transformed stamens (third whorl), and in ovules primordia when the carpels began to fuse (Fig. 4G).

To corroborate that the *sl* mutations found at the *TAP3* gene and the decrease of transcript level were responsible for the mutant phenotypes, *sl-Pr* and *sl-LA0269* mutants were compared with *TAP3* antisense lines varying in silencing level. All *TAP3* antisense lines showed abnormal phenotypes affecting flower development, most of which resembled those of the *sl-LA0269* mutant, whereas the stronger ones were similar to those of the *sl-Pr* mutant. At anthesis, flowers from *TAP3* antisense lines showed a variable degree of homeotic conversion both for petals into sepals in the second whorl and stamens into carpels in the third whorl (Fig. 5A). Interestingly, phenotype features of the antisense line numbers 28 (extreme conversions) and 32 (partial conversions) indicated that severity of homeotic changes were correlated to the silencing level of the *TAP3* gene (Fig. 5B). In addition, parthenocarpic fruits to which carpeloid stamens remained attached were observed during antisense fruit ripening (Fig. 5D, E compared to Fig. 5C). Phenotypic alterations affecting the vegetative growth were not found.

Transcriptional regulation of floral organ identity genes in the stamenless *mutants*

We investigated whether the strong *sl-Pr* mutation affected other floral organ identity genes by analysing the expression of tomato ABC genes in WT and *sl-Pr* inflorescences during flower development (Fig. 6). The most significant differences concerned the A-class *MC* gene. The *MC* transcript level was significantly higher in mutants than in WT plants in both young flower and flowers at anthesis (Fig. 6). The expression level of the B-class genes *TPI*, *TPIB*, and *TM6*

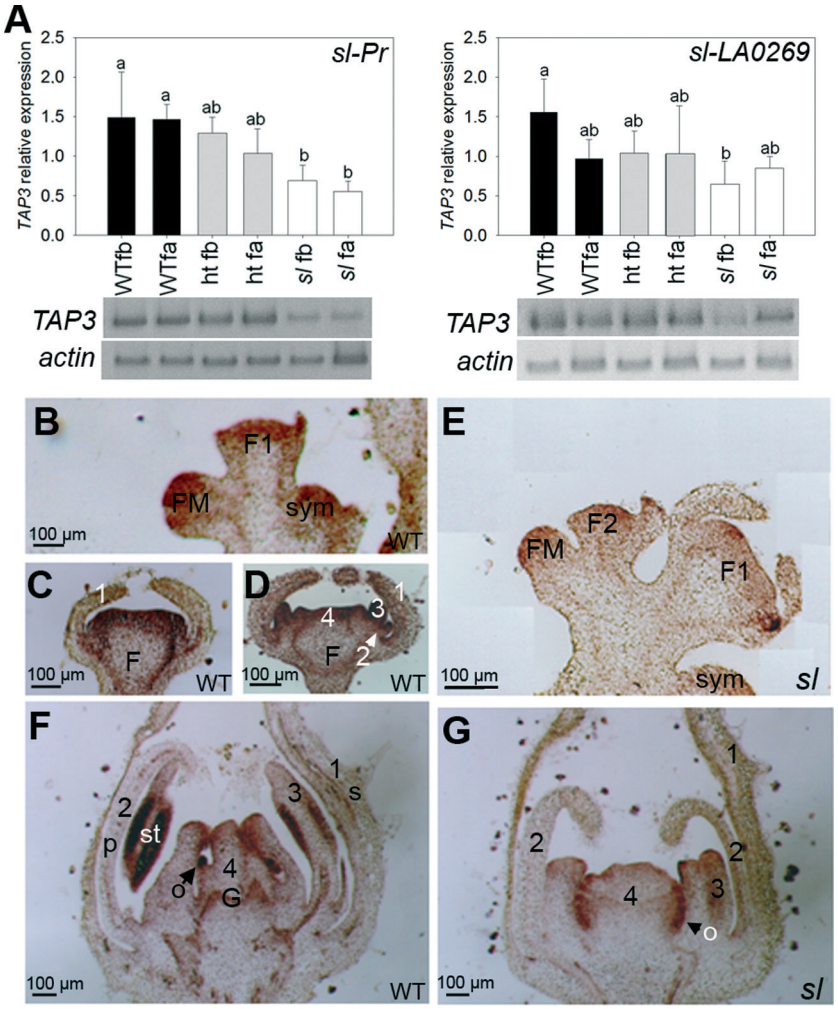

Fig. 4. Expression of *STAMENLESS* (*SL*, *TAP3*) during flower development in *stamenless* tomato mutants. (A) Semi-quantitative RT-PCR expression in the WT plants, heterozygote plants (ht) and mutant (*sl*) plants in green flower buds of ≈5 mm length (fb) and flowers at anthesis (fa) for both *sl-Pr* and *sl-LA0269* mutations. Actin transcripts were used as a PCR control. *TAP3* relative expression level compared to actin was analyzed by gel densitometry. Values followed by a same letter (a, b) are not statistically different ($P < 0.01$). (B–G) Tissue localization of transcripts by means of *in situ* hybridization (*SL* antisense probe) in WT and *sl-LA0269* mutant. (B) WT young inflorescence carrying flower buds and floral meristem, (C, D) flower buds from WT plants initiating floral organ primordia, (E) *sl* mutant young inflorescence carrying several flower buds initiating floral organ primordia and a floral meristem. (F), WT flower just after fusion of the carpels, (G) *sl* mutant flower before fusion of the carpels. 1–4, floral primordia or organs of first, second, third, or fourth floral whorls; F, flower; FM, floral meristem; G, gynoecium; o, ovules; p, petal; s, sepal; st, stamen; sym, sympodial meristem.

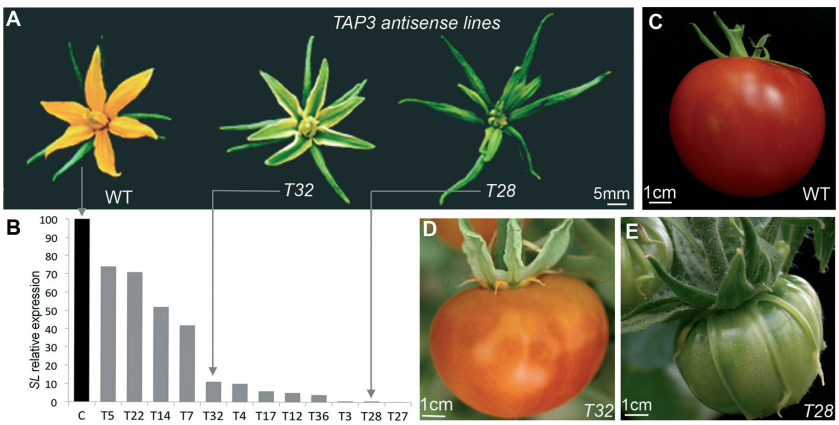

Fig. 5. Floral and fruit phenotypes of the WT tomato and *TAP3 antisense lines*. (A) WT flower (left) and *TAP3 antisense* flowers (T32 and T28) showing different degrees of conversion for petals into sepals and stamens into carpels. (B) *SL* (*TAP3*) expression level in *TAP3 antisense* lines relative to WT (C). The phenotype of the antisense lines in (A) was correlated to the silencing level of the *TAP3* gene in (B) (grey arrows). (C–E) WT fruits with the sepals of whorl 1 remaining attached to the fruit (C) and parthenocarpic fruits of *TAP3* antisense lines T32 (D) and T28 (E) with the sepals of whorl 1 and modified organs of whorls 2 and 3 remaining attached to the fruit depending on the phenotype.

was not significantly affected by the *sl-Pr* mutation during flower development (Fig. 6). The transcript level of the C-class (*TAG1*) and E-class (*TM5* and *TAGL2*) genes here analysed were also similar in WT and mutant plants (Fig. 6).

Effects of GA and IAA hormone treatments on the stamenless *flower phenotype*

Because GA_3 could play a role in the *sl-LA0269* mutant phenotype reversion (Gómez *et al.*, 1999), we tested whether the stronger *sl-Pr* phenotype could also be reverted by hormonal applications to highlight the link between *SL* and phytohormones in petal and stamen development. In Pr plants, GA_3 and IAA treatments did not modify floral organ identity (Table S1): GA_3-treated Pr stamens and carpels (Fig. 7 G, H) were similar to the control ones (Fig. 7 A–C) and the same happened in IAA-treated Pr flowers. In the same way, no floral organ modifications were observed in *sl-Pr* mutant plants in response to 0.5 mM GA_3 compared to controls (Table S1). However, a partial reversion of three to six carpels per flower into pseudo-stamens was observed in the third whorl of around half the flowers treated with 1 mM GA_3 (Fig. 7I, J compared to Fig. 7 D, E). Most reverted flowers produced pollen grains, although pollen viability was lower (52.3%) than it was in WT flowers (91.2%). Moreover, non-fused carpelloid organs bearing external ovules were observed on whorl 3 in around half the 1 mM GA_3-treated *sl-Pr* flowers. Mutant plants treated with IAA produced twisted gynoecium and whorl 3 non-fused carpelloid organs with external ovules were observed in a third of the plants (Fig. 7K) but the abnormal third-whorl structures never produced pollen. We also observed ABC gene expression in WT and *sl-Pr* inflorescences after hormonal treatment, but neither the 1 mM IAA nor the 1 mM GA_3 treatment markedly affected gene expression (Fig. 7L).

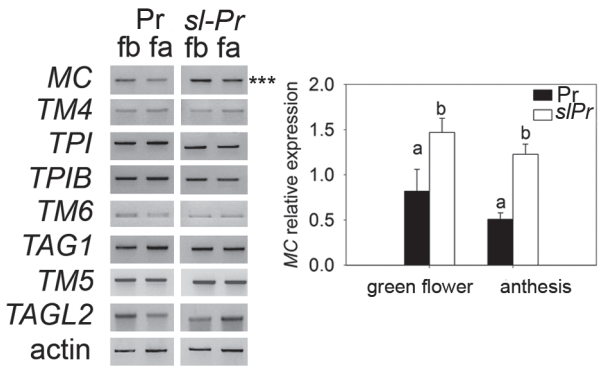

Fig. 6. Semi-quantitative RT-PCR expression analysis of tomato floral organ identity genes in Pr and *sl-Pr* mutant flowers along with their development: green flower buds of ≈5 mm length (fb) and flowers at anthesis (fa). Actin transcripts were used as a PCR control. Significant differences between genotypes according to ANOVA are indicated ($P < 0.001$***). For observed significant differences, relative expression levels in relation to actin are graphically presented. *MACROCALYX* (*MC*) relative expression level was analysed by gel densitometry. On the graph, matching letters (a, b) are not statistically different ($P < 0.001$).

Endogenous phytohormone concentrations in stamenless *mutant*

To further investigate whether the *sl* mutation affects phytohormone content, we quantified endogenous phytohormone concentrations in the strong *sl-Pr* mutant during inflorescence development. Most hormone concentrations varied with

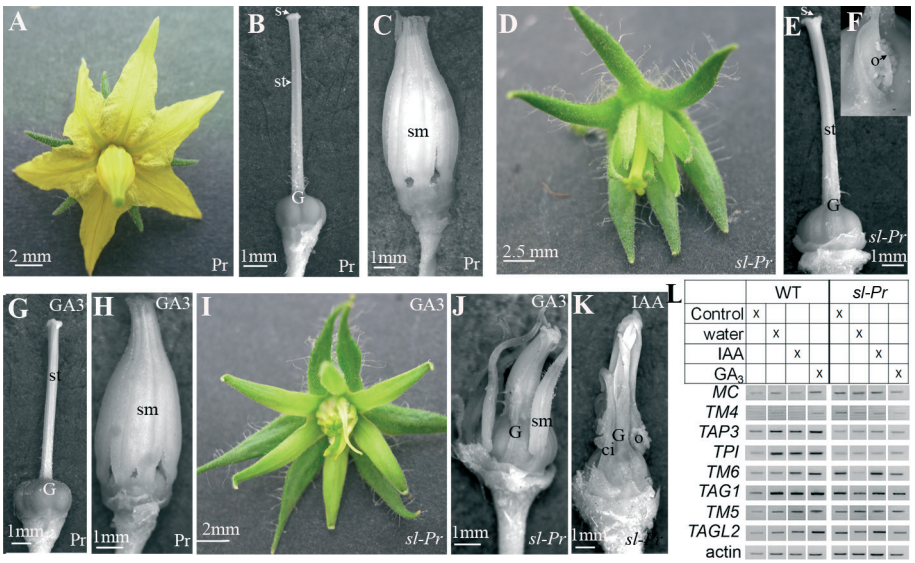

Fig. 7. Hormonal treatment impacts on the flowers of the *stamenless* (*sl-Pr*) tomato mutant. (A–C) Water-treated (control) Pr flowers with normal (B) gynoecium and (C) stamens. (D–F) *sl-Pr* mutant flowers treated with water (control) showing (D) sepals in the second floral whorl and (E) gynoecium resulting from the fusion of the carpels of third and fourth floral whorls, (F) some external ovules could be observed on some non-fused carpels. (G, H) Pr flowers treated with 1 mM GA_3 with normal (G) gynoecium and (H) stamens. Note that similar pictures were obtained for Pr flowers treated with 1 mM IAA. (I, J) *sl-Pr* mutant flowers treated with 1 mM GA_3 showing a partial reversion of the third floral whorl organs in (J) stamens. (K) *sl-Pr* mutant flowers treated with 1 mM IAA showing a gynoecium with non-fused carpels and external ovules. ci, non-fused carpel; G, gynoecium; o, external ovules; s, stigma; sm, stamen; st, style. (L) Semi-quantitative RT-PCR expression analysis of tomato floral organ identity genes in WT and *sl-Pr* inflorescences at anthesis treated with water, 1 mM IAA, or 1 mM GA_3. Actin transcripts were used as the PCR control.

inflorescence stage and were reduced in the *sl-Pr* mutant (Figs 8 and 9). Indeed, the *sl-Pr* mutation showed decreased GA and auxin concentrations relative to the WT plants (Fig. 8A, B). Both contents tend to decrease after anthesis while CK content showed an overall increase associated with the flower developmental stage (Fig. 8C–F). The effect of the *sl-Pr* mutation varied with respect to the CK classes; it reduced the contents of bioactive CKs (free bases and ribosides) and CK glucoconjugates (Fig. 8C–E) and increased the CK phosphate concentrations in the flower at anthesis (Fig. 8F). With respect to the ethylene precursor ACC we observed a significant reduction in *sl-Pr* floral buds and pre-anthesis flowers compared to the WT blooms but not in the flowers at anthesis (Fig. 8G). The BzA concentration was higher in *sl-Pr* relative to *Pr* in inflorescence buds but the difference was no more visible at later flower developmental stages (Fig. 8H). The JA concentration was clearly enhanced by the *sl-Pr* mutation at all developmental stages (Fig. 9A). The concentrations of both SA (Fig. 9B) and Brs (Fig. 9C) increased with inflorescence development primarily in the Pr; however, the SA level was

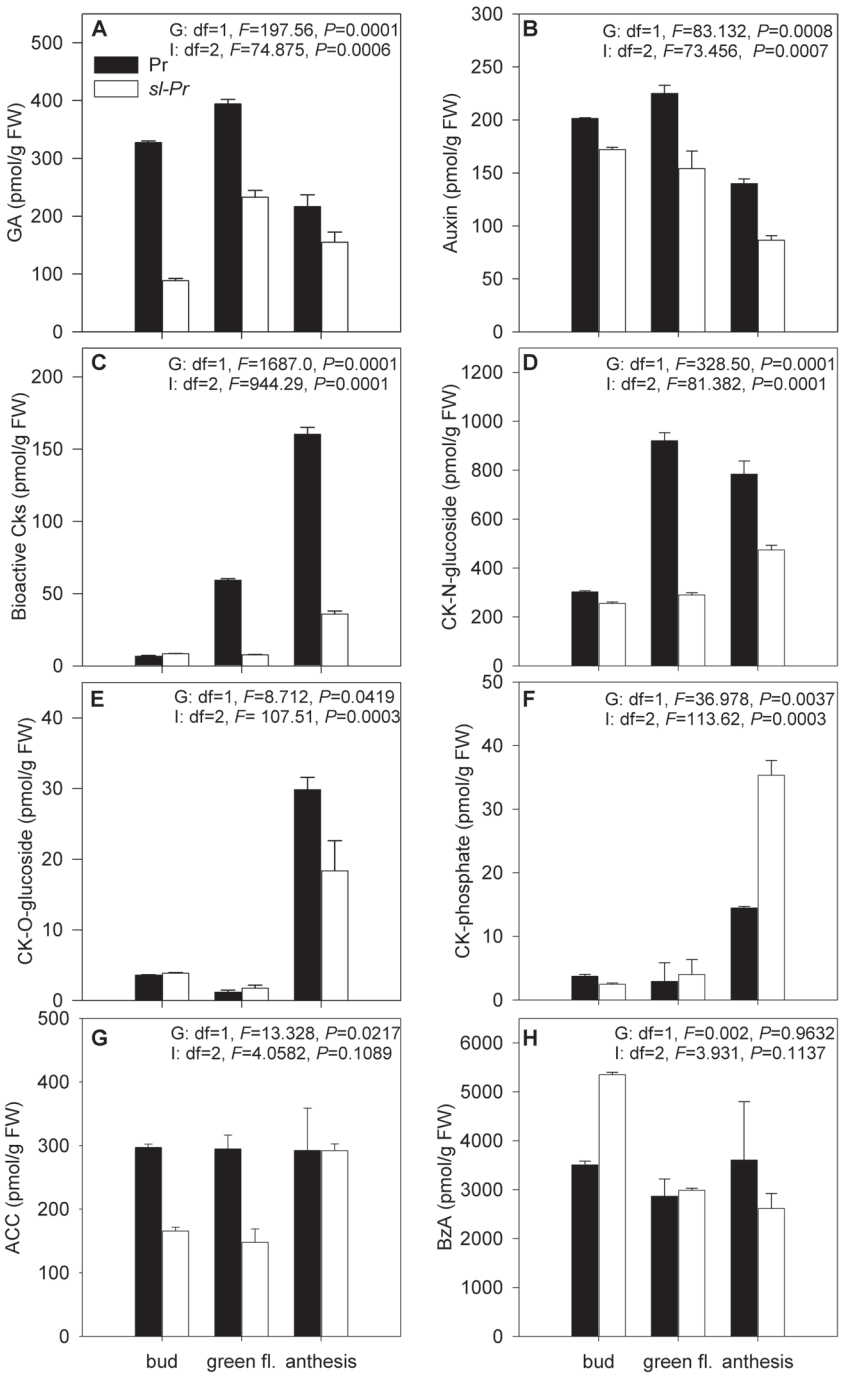

Fig. 8. Impact of the *stamenless* (*sl-Pr*) tomato mutation on endogenous phytohormone content. (A) Gibberellins (GA), (B) auxin; (C) bioactive CKs, (D) CK-*N*-glucosides, (E) CK-*O*-glucosides, (F) CK phosphates, (G) ethylene precursor ACC, and (H) benzoic acid (BzA) during flower development (developmental stages: flower buds <5 mm length, green flowers before anthesis ≈5–8 mm length, flowers at anthesis). Bars = SD; ANOVA II results for the genotype (G) and inflorescence stage (I) factors are presented.

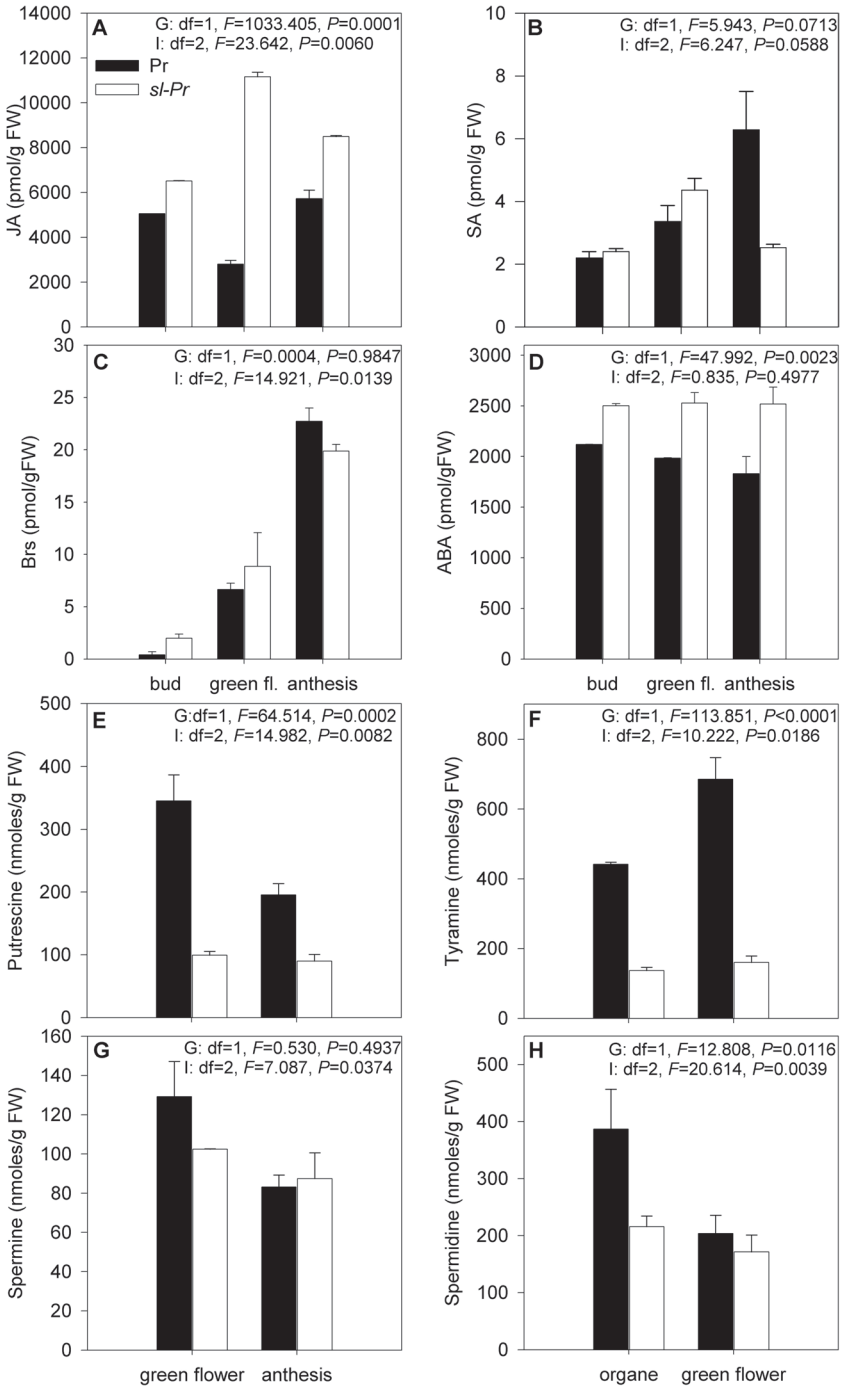

Fig. 9. Impact of the *stamenless* (*sl-Pr*) tomato mutation on endogenous phytohormones and PA contents. (A) JA, (B) SA, (C) Brs, (D) ABA, and (E–H) PAs (E, putrescine; F, tyramine; G, spermine; H, spermidine) contents during flower development (developmental stages: flower buds <5 mm length, green flowers before anthesis ≈5–8 mm length, flowers at anthesis). Bars = SD; ANOVA II results for the genotype (G) and inflorescence stage (I) factors are presented.

lowered in the mutant flowers at anthesis compared to the WT (Fig. 9B) while the *sl-Pr* mutation did not significantly affect Brs content (Fig. 9C). The total ABA content was higher in *sl-Pr* compared to the WT whatever the developmental stage (Fig. 9D). In general, the PA concentration decreased during inflorescence development (Fig. 9E–H). The spermidine, tyramine, and putrescine concentrations were lower in mutant inflorescences than in WT ones even though the difference was not significant for spermidine in flowers at anthesis (Fig. 9E, F, H), but the overall spermine concentration was not affected by the genotype (Fig. 9G).

Discussion

stamenless *mutations affect B-class gene* TAP3

Several tomato mutants have been described with various degrees of petal conversion into sepals and stamens

into carpels (Hafen and Stevenson, 1958; Nash *et al.*, 1985; Philouze, 1991; Rasmussen and Green, 1993; Gómez *et al.*, 1999), but the underlying genes have not yet been formally identified. Four B-class genes are known in tomato, the *AP3* homologues *TAP3* and *TM6* and the *PI* homologues *TPI* and *TPIB* (Pnueli *et al.*, 1991; Busi *et al.*, 2003; de Martino *et al.*, 2006; Mazzucato *et al.*, 2008; Geuten and Irish, 2010). The *SL* locus has been suggested as the tomato orthologue of B-function *DEF* gene of *Antirrhinum majus* and *AP3* of *Arabidopsis* (Gómez *et al.*, 1999; Mazzucato *et al.*, 2008). Both *SL* and *TAP3* map on the long arm of chromosome 4 while the remaining tomato B-class genes map in different chromosomes; that is, *TM6* on chromosome 2, *TPI* on chromosome 6, and *TPIB* on chromosome 8 (Khush, 1965; Mazzucato *et al.*, 2008; Olimpieri and Mazzucato, 2008). In this study we identified the mutation in the *TAP3* promoter region of the *sl-LA0269* mutant and described the TAP3 truncated protein encoded by the *TAP3* mutant allele of the *sl-Pr* mutant genome. We have also proved that both mutations were allelic and evidenced that the phenotype showed by homozygous *sl* mutant plants were identical, or very similar, to those of *TAP3* antisense lines. Moreover, the strong phenotype of the *sl-Pr* mutant was in accordance with a knock-out mutation in the *TAP3* gene. *TAP3* loss-of-function mutants indeed showed a complete conversion of petals into sepals and of stamens into carpels while *TM6*, *TPI*, and *TPIB* loss-of-function mutations affected mainly or exclusively stamen identity (de Martino *et al.* 2006; Geuten and Irish, 2010). Together these results provide clear evidence indicating that the *SL* locus corresponds to the *TAP3* gene of tomato.

The intensity of the *sl* phenotypes could depend on the *TAP3* expression level as suggested by the observed *TAP3* antisense lines and the *sl-LA0269* mutant and could explain the incomplete dominance observed in the heterozygote plants (Figs 4 and 5). However, even if *TAP3* is still weakly expressed in the *sl-Pr* mutant, it exhibits a strong phenotype similar to that of the *TAP3* loss-of-function mutant (de Martino *et al.*, 2006), suggesting that the truncated protein may not be functional as the mutation affected a protein region important for the correct specification of petal and stamen identity. The lost of half of the K box domain of the TAP3 protein in *sl-Pr* mutant plants most likely affect the capacity of this *sl-Pr* truncated protein to form multimeric MADS complex since interactions between MADS domain proteins are largely achieved via the K domain (Leseberg *et al.*, 2008). The consequence of the loss of the C-terminal domain of TAP3 truncated protein is not clear since its molecular role is not well understood (Geuten and Irish, 2010).

Regulation of the ABC genes by STAMENLESS

Phenotypic and genetic analyses performed in this work indicated that *stamenless* mutations affected the *TAP3* gene. In addition, molecular characterization of *SL* has revealed it is a key regulator of the development of petal and stamen organs, as expected for an *AP3* orthologous gene. It is known that TAP3 protein participates in the formation of multimeric MADS complexes regulating petal and stamen development (de Martino *et al.*, 2006; Leseberg *et al.*, 2008; Geuten and Irish, 2010), although the composition of such complexes and their organ specificity require additional research in tomato plants (Smaczniak *et al.*, 2012). In this paper, we have investigated the interactions between *TAP3* and the remaining tomato B-class genes involved in flower development.

According to our results, the *sl-Pr* mutation did not markedly modify the expression of *TM6*, *TPI*, and *TPIB* in flowers indicating that the mutant flower phenotype is not due to a coordinated misregulation of *TAP3*, *TM6*, *TPI*, and *TPIB*. Most likely, the *sl-Pr* mutation must be sufficient to prevent the formation of functional complexes determining petal and stamen identity. Previous studies by de Martino *et al.* (2006) also showed that a *tap3* knock-out mutation did not modify the expression of *TM6* and *TPI* in tomato flowers and that *TM6* inactivation did not affect *TAP3* and *TPI* expression. However, Geuten and Irish (2010) reported interactions between B-class genes in tomato floral organs and showed that expression of *TPI* and *TPIB* was completely absent in second- and third-whorl organs of *tap3* knock-out mutants. They also reported that *TAP3* expression increased in *TPIB* RNAi plants and decreased in *TPI* RNAi flowers compared to WT and that cross-activation of *TPI* and *TPIB* took place in the second-whorl organs (Geuten and Irish, 2010). Additional experiments would be required to explain these differences in the regulatory interactions mediated by *TAP3* gene. However, the possibility that *TAP3* regulates *TPI* and *TPIB* expression in a similar way to *AP3* is required for the maintenance of *PI* gene expression during flower morphogenesis in *Arabidopsis* (Goto and Meyerowitz, 1994; Honma and Goto, 2000) might be studied in detail.

Among the other floral organ identity genes, our results showed that the *sl-Pr* mutation did not significantly affect the expression of C- and E-class genes, but it increased *MC* transcript levels, suggesting that *TAP3* may be involved in the repression of class A gene *MC*. Similarly, Sundström *et al.* (2006) observed increased *AP1* expression in the *ap3* mutant of Arabidopsis, and their results suggested a direct *AP1* regulation by the AP3/PI dimer. However, a putative regulation of *MC* by complexes containing TAP3 requires further investigation.

Hormonal regulation of flower development is mediated by STAMENLESS

It has been shown that low temperatures and/or GA treatment may partly revert the floral phenotype of the weak allelic *stamenless* mutants *sl-LA0269* and *sl-2* (Sawhney 1983; Gómez *et al.* 1999), suggesting a role for phytohormones in the development of tomato floral organs. We investigated whether hormonal applications could also reverse the complete second- and third-whorl organs conversion of the strong *sl-Pr* mutant. We indeed observed a partial reversion of the third-whorl organs of the *sl-Pr* mutant in response to 1 mM GA_3, but a higher concentration was required to induce reversion in *sl-Pr* relative to *sl-LA0269* (Gómez *et al.*, 1999). Moreover, according to previous reports (Sawhney, 1983; Sawhney and Greyson, 1973b), IAA strengthens the *sl-2* mutant phenotype. Our results showed that IAA affected the flower development

in the *sl-Pr* mutant but in a different way compared to *sl-2* since it increased the development of abnormal carpels in the third floral whorl in *sl-Pr*. However, according to our results, neither IAA nor GA_3 strongly affected the ABC gene expression in *sl-Pr*, suggesting that the partial reversion of the mutant does not rely on an upstream regulation of the floral meristem identity genes by hormones and that phytohormones most likely act downstream of the ABC genes at this floral stage in tomato. However, Yu *et al.* (2004) showed that GA promotes normal floral organ development in *Arabidopsis* by partly up-regulating the expression of the B- and C-function floral genes, but it did not regulate A-function genes.

The modified phytohormone profile in *sl-Pr* inflorescences provides further arguments for a phytohormone role in the floral organ development downstream of the *SL* gene in tomato. We indeed showed that the *sl-Pr* mutation reduced GA, IAA, most classes of CKs (bioactive and glycosylated forms), ACC, SA, spermine, and tyramine concentrations and increased JA and ABA in flowers. The lower concentrations of GA and IAA were consistent with the fact that an exogenous application of GA_3 and IAA (in a less extent) may partly rescue the flower phenotype of the mutant. Modified phytohormone profiling was also observed in the *sl-2* mutant (Sawhney 1974; Rastogi and Sawhney, 1990; Singh *et al.*, 1992; Singh and Sawhney, 1998). A regulation of phytohormones downstream of the floral organ identity genes has been demonstrated in other species. In *Arabidopsis*, recent genomic studies showed that floral homeotic proteins bind thousands of target genes and that genes involved in the transcriptional control and hormone functions feature prominently among the early and direct targets (Chandler, 2011; Ito, 2011; Sablowski, 2010). Mutant and gene characterization studies in *Arabidopsis* have shown that stamen development is reliant on almost all hormones, petal development is affected by GAs, auxins, and JA, and gynoecium development is predominantly regulated by auxins (Chandler, 2011). Our results argue for a similar hormonal regulation of stamens and petals in tomato. We indeed showed a modification in most phytohormones in response to the *sl-Pr* mutation during flower development and the abnormal petals and stamens in the *sl2* mutant was at least partly related to elevated levels of endogenous PAs, IAA, and ABA and to the reduction in GA levels (; Sawhney 1974; Rastogi and Sawhney, 1990Singh *et al.*, 1992; Singh and Sawhney, 1998). A decrease in GA levels was often associated with stamen development defects in tomato. GA-deficient tomato mutants *gib-1* and *ga-2* exhibit abnormal flowers with arrested anther development (Nester and Zeevart, 1988; Jacobsen and Olszewski, 1991). The silencing of *GA20-oxidase 1* was also shown to be detrimental for pollen production (Olimpieri *et al.*, 2011). PA involvement in flower development was also reported in the tomato *pat* mutant, which exhibits aberrations in stamen development and female fertility and showed changes in the different PA contents relative to the WT (Antognonia *et al.*, 2002). How floral organs identity genes affect genes involved in hormone synthesis and perception remains to be investigated in tomato.

Notable progress has been made in understanding phytohormone function in floral development, and it is clear that male development in particular is regulated by multiple hormones in concert. However, further investigation is required to understand the complex network between phytohormone pathways, floral organ identity genes, and flower-building genes in different plant species.

Supplementary material

Supplementary material is available at *JXB* online.

Supplementary Table S1. Hormonal treatment impact on the number of organs and on the organ size per whorl in WT tomato (Pr) and in the *stamenless* (*sl-Pr*) mutant.

Acknowledgements

The authors thank Marie Korecká for invaluable technical support in providing phytohormone analyses. This research was supported by the Belgian 'Fonds de la Recherche Scientifique' (crédit aux chercheurs 1.5.101.08.F), the Spanish Ministry of Economy and Competitiveness (grant BIO2009-11484), and the Czech Science Foundation (grant P506/11/0774). The authors also thank the Campus de Excelencia Internacional Agroalimentario (CeiA3) for supporting this research collaboration.

References

Alexander MP. 1969. Differential staining of aborted and non-aborted pollen. *Biotechnic and Histochemistry* **44,** 117–122.

Ampomah-Dwamena C, Morris BA, Sutherland P, Veit B, Yao JL. 2002. Down-regulation of *TM29*, a tomato *SEPALLATA* homolog, causes parthenocarpic fruit development and floral reversion. *Plant Physiology* **130,** 605–617.

Antognonia F, Ghettia F, Mazzucato A, Franceschettia M, Bagnia N. 2002. Polyamine pattern during flower development in the *parthenocarpic fruit* (*pat*) mutant of tomato. *Physiologia Plantarum* **116,** 539–547.

Baulcombe DC, Saunders GR, Bevan MB, Harrison BD. 1986. Expression of biologically active viral satellite RNA from the nuclear genome of transformed plants. *Nature* **321,** 446–449.

Bishop CJ. 1954. A *stamenless* male-sterile tomato. *American Journal of Botany* **4,** 540–542.

Brukhin V, Hernould M, Gonzalez N, Chevalier C, Mouras A. 2003. Flower development schedule in tomato *Lycopersicon esculentum* cv. sweet cherry. *Sexual Plant Reproduction* **15,** 311–320.

Busi MV, Bustamante C, D'Angelo C, Hidalgo-Cuevas M, Boggio SB, Valle EM, Zabaleta E. 2003. MADS-box genes expressed during tomato seed and fruit development. *Plant Molecular Biology* **52,** 801–815.

Chandler JW. 2011. The hormonal regulation of flower development. *Journal of Plant Growth Regulation* **30,** 242–254.

Coen ES, Meyerowitz EM. 1991. The war of the whorls, genetic interactions controlling flower development. *Nature* **353,** 31–37.

Colombo L, Franken J, Koetje E, van Went J, Dons HJ, Angenent GC, van Tunen AJ. 1995. The petunia MADS box gene *FBP11* determines ovule identity. *The Plant Cell* **7,** 1859–1868.

de Martino G, Pana I, Emmanuel E, Levy A, Vivian F, Irish VF. 2006. Functional analyses of two tomato *APETALA3* genes demonstrate diversification in their roles in regulating floral development. *The Plant Cell* **18,** 1833–1845.

Djilianov DL, Dobrev PI, Moyankova DP, Vankova R, Georgieva DT, Gajdosova S, Motyka V. 2013. Dynamics of endogenous phytohormones during desiccation and recovery of the resurrection plant species *Haberlea rhodopensis*. *Journal of Plant Growth Regulation* **32,** 564–574.

Dobrev PI, Kamínek M. 2002. Fast and efficient separation of cytokinins from auxin and abscisic acid and their purification using mixed-mode solid-phase extraction. *Journal of Chromatography A* **950,** 21–29.

Dobrev PI, Vankova R. 2012. Quantification of abscisic acid, cytokinin, and auxin content in salt-stressed plant tissues. In: Shabala S, Ann Cuin T, eds. *Plant Salt Tolerance: Methods and Protocols, Methods in Molecular Biology, vol. 913*. Berlin: Springer Science + Business Media, pp 251–261.

Ellul P, Angosto T, García-Sogo B, García-Hurtado N, Martín-Trillo M, Salinas M, Moreno V, Lozano R, Martínez-Zapater JM. 2004. Expression of *Arabidopsis APETALA1* in tomato reduces its vegetative cycle without affecting plant production. *Molecular Breeding* **13,** 155–163.

Geuten K, Irish V. 2010. Hidden variability of floral homeotic B genes in Solanaceae provides a molecular basis for the evolution of novel functions. *The Plant Cell* **22,** 2562–2578.

Giménez E, Pineda B, Capel J, Antón MT, Atarés A, Pérez-Martín F, García-Sogo B, Angosto T, Moreno V, Lozano R. 2010. Functional analysis of the *arlequin* mutant corroborates the essential role of the *ARLEQUIN/TAGL1* gene during reproductive development of tomato. *PLoS ONE* **5,** e14427.

Gómez P, Jamilena M, Capel J, Zurita S, Angosto T, Lozano R. 1999. *Stamenless*, a tomato mutant with homeotic conversions in petals and stamens. *Planta* **209,** 172–179.

Goto K, Meyerowitz EM. 1994. Function and regulation of the Arabidopsis floral homeotic gene *PISTILLATA. Genes and Development* **8,** 1548–1560.

Hafen L, Stevenson EC. 1958. Preliminary studies on five *stamenless* mutants. *Tomato Genetics Cooperative Reports* **8,** 17–18.

Hernandez-Hernandez T, Martinez-Castilla LP, Alvarez-Buylla ER. 2007. Functional diversification of B MADS-box homeotic regulators of flower development: adaptive evolution in protein-protein interaction domains after major gene duplication events. *Molecular Biology and Evolution* **24,** 465–481.

Honma T, Goto K. 2000. The Arabidopsis floral homeotic gene *PISTILLATA* is regulated by discrete cis-elements responsive to induction and maintenance signals. *Development* **127,** 2021–2030.

Ito T. 2011. Coordination of flower development by homeotic master regulators. *Current Opinion in Plant Biology* **14,** 53–59.

Jacobsen SE, Olszewski NE. 1991. Characterization of the arrest in anther development associated with gibberellin deficiency of the *gib-1* mutant of tomato. *Plant Physiology* **97,** 409–414.

Kaufmann K, Muiño JM, Jauregui R, Airoldi CA, Smaczniak C, Krajewski P, Angenent GC. 2009. Target genes of the MADS transcription factor *SEPALLATA3:* integration of developmental and hormonal pathways in the Arabidopsis flower. *PLoS Biology* **7,** e1000090.

Khush GS. 1965. Linkage analysis of chromosome 4. *Tomato Genetics Cooperative Reports* **15,** 35.

Kramer EM, Dorit RL, Irish VF. 1998. Molecular evolution of petal and stamen development, Gene duplication and divergence within the *APETALA3* and *PISTILLATA* MADS-box gene lineages. *Genetics* **149,** 765–783.

Lefèvre I, Gratia E, Lutts S. 2001. Discrimination between the ionic and osmotic components of salt stress in relation to free polyamine level in rice (*Oryza sativa*). *Plant Science* **161,** 943–952.

Leseberg CH, Eissler CL, Wang X, Johns MA, Duvall MR, Mao L. 2008. Interaction study of MADS-domain proteins in tomato. *Journal of Experimental Botany* **59,** 2253–2265.

Lozano R, Angosto T, Gómez P, Payan C, Capel J, Huijser P, Salinas J, Martinez-Zapater JM. 1998. Tomato flower abnormalities induced by low temperatures are associated with changes of expression of MADS-box genes. *Plant Physiology* **117,** 91–100.

Lozano R, Gimenez E, Cara B, Capel J, Angosto T. 2009. Genetic analysis of reproductive development in tomato. *International Journal of Developmental Biology* **53,** 8–10.

Mazzucato A, Olimpieri I, Siligato F, Picarella ME, Soressi GP. 2008. Characterization of genes controlling stamen identity and development in a parthenocarpic tomato mutant indicates a role for the *DEFICIENS* ortholog in the control of fruit set. *Physiologia Plantarum* **132,** 526–537.

Nash AF, Gardner RG, Henderson WR. 1985. Evaluation of allelism and seed set of eight *stamenless* tomato mutants. *Horticultural Science* **20,** 440–442.

Nester JE, Zeevaart JAD. 1988. Flower development in normal tomato and a gibberellin-deficient (*ga-2*) mutant. *American Journal of Botany* **75,** 45–55.

Olimpieri I, Mazzucato A. 2008. Phenotypic and genetic characterization of the *pistillate* mutation in tomato. *Theoretical and Applied Genetics* **118,** 151–163.

Olimpieri I, Caccia R, Picarella ME, Pucci A, Santangelo E, Soressi GP, Mazzucato A. 2011. Constitutive co-suppression of the *GA 20-oxidase1* gene in tomato leads to severe defects in vegetative and reproductive development. *Plant Science* **180,** 496–503.

Pelaz S, Tapia-Lopez R, Alvarez-Buylla ER, Yanofsky MF. 2001. Conversion of leaves into petals in Arabidopsis. *Current Biology* **11,** 182–184.

Philouze J. 1991. Description of isogenic lines, except for one, or two, monogenetically controlled morphological traits in tomato, *Lycopersicon esculentum* Mill. *Euphytica* **56,** 121–131.

Pnueli L, Abu-Abeid M, Zamir D, Nacken W, Schwarzsommer Z, Lifschitz E. 1991. The MADS box gene family in tomato: temporal expression during floral development, conserved secondary structures and homology with homeotic genes from Antirrhinum and Arabidopsis. *The Plant Journal* **1,** 255–266.

Pnueli L, Hareven D, Broday L, Hurwitz C. 1994b. The *TM5* MADS box gene mediates organ differentiation in the three inner whorls of tomato flowers. *The Plant Cell* **6,** 175–186.

Pnueli L, Hareven D, Rounsley SD, Yanofsky MF. 1994a. Isolation of the tomato *AGAMOUS* gene *TAG1* and analysis of its homeotic role in transgenic plants. *The Plant Cell* **6,** 163–173.

Rasmussen N, Green PB. 1993. Organogenesis in flowers of the homeotic *green pistillate* mutant of tomato (*Lycopersicon esculentum*). *American Journal of Botany* **80,** 805–813.

Rastogi R, Sawhney VK. 1990. Polyamines and flower development in the male sterile *stamenless-2* mutant of tomato (*Lycopersicon esculentum* Mill.): I. Level of polyamines and their biosynthesis in normal and mutant flowers. *Plant Physiology* **93,** 439–445.

Sablowski R. 2010. Genes and functions controlled by floral identity genes. *Seminars in Cell and Developmental Biology* **21,** 94–99.

Sawhney VK. 1974. Morphogenesis of the *stamenless-2* mutant in tomato. III. Relative levels of gibberellins in the normal and mutant plants. *Journal of Experimental Botany* **25,** 1004–1009.

Sawhney VK. 1983. The role of temperature and its relationship with gibberellic acid in the development of floral organs of tomato (*Lycopersicum esculentum*). *Canadian Journal of Botany* **61,** 1258–1265.

Sawhney VK, Greyson RI. 1973a. Morphogenesis of the *stamenless-2* mutant in tomato. I. Comparative description of the flowers and ontogeny of stamens in the normal and mutant plants. *American Journal of Botany* **60,** 514–523.

Sawhney VK, Greyson RI. 1973b. Morphogenesis of the *stamenless-2* mutant in tomato. I. Modifications of sex organs in the mutant and normal flowers by plant hormones. *Canadian Journal of Botany* **51,** 2473–2479.

Schupp JM, Price LB, Klevytska A, Keim P. 1999. Internal and flanking sequence from AFLP fragments using ligation-mediated suppression PCR. *BioTechniques* **26,** 905–912.

Singh S, Sawhney VK. 1998. Abscisic acid in a male sterile tomato mutant and its regulation by low temperature. *Journal of Experimental Botany* **49,** 199–203.

Singh S, Sawhney VK, Pearce DW. 1992. Temperature effects on endogenous indole-3-acetic acid levels in leaves and stamens of the normal and male sterile '*stamenless-2*' mutant of tomato (*Lycopersicon esculentum* Mill.). *Plant, Cell and Environment* **15,** 373–377.

Smaczniak C, Immink RGH, Angenent GC, Kaufmann K. 2012. Developmental and evolutionary diversity of plant MADS domain factors: insights from recent studies. *Development* **139,** 3081–3098.

Sundström JF, Nakayama N, Glimelius K and Irish VF. 2006. Direct regulation of the floral homeotic *APETALA1* gene by APETALA3 and PISTILLATA in Arabidopsis. *The Plant Journal* **46,** 593–600.

Theissen G, Becker A, Di Rosa A, Kanno A, Kim JT, Muenster T, Winter KW, Saedler H. 2000. A short history of MADS-box genes in plants. *Plant Molecular Biology* **42,** 115–149.

Vrebalov J, Ruezinsky D, Padmanabhan V, White R, Medrano D, Drake R, Schuch W, Giovannoni J. 2002. A MADS-box gene necessary for fruit ripening at the tomato *ripening-inhibitor* (*rin*) locus. *Science* **296,** 343–346.

Vrebalov J, Pan IL, Arroyo AJM, McQuinn R, Chung M, Poole M, Rose J, Seymour G, Grandillo S, Giovannoni J, Irish VF. 2009. Fleshy fruit expansion and ripening are regulated by the tomato *SHATTERPROOF* Gene *TAGL1*. *The Plant Cell* **21,** 3041–3062.

Yu H, Ito T, Zhao Y, Peng J, Kumar P, Meyerowitz EM. 2004. Floral homeotic genes are targets of gibberellins signalling in flower development. *Proceedings of the National Academy of Sciences, USA* **101,** 7827–7832.